International Journal of Applied Earth Observation and Geoinformation 21 (2013) 53–65

Contents lists available at SciVerse ScienceDirect

International Journal of Applied Earth Observation and Geoinformation

journal homepage: www.elsevier.com/locate/jag

Modelling the spectral response of the desert tree *Prosopis tamarugo* to water stress

R.O. Chávez[a,*], J.G.P.W. Clevers[a], M. Herold[a], M. Ortiz[c,b], E. Acevedo[b]

[a] *Laboratory of Geo-Information Science and Remote Sensing, Wageningen University, P.O. Box 47, 6700 AA Wageningen, The Netherlands*
[b] *Laboratorio de Relación Suelo-Agua-Planta, Facultad de Ciencias Agronómicas, Universidad de Chile, Casilla 1004, Santiago, Chile*
[c] *Centro de Estudios Avanzados en Fruticultura (CEAF), Conicyt-Regional R08I1001, Av. Salamanca s/n, Rengo, Chile*

ARTICLE INFO

Article history:
Received 15 June 2012
Accepted 22 August 2012

Keywords:
Arid ecosystems
Radiative transfer model
Soil-Leaf-Canopy
Water stress
Spectral reflectance
Vegetation indices
Remote sensing
Tamarugo
Atacama

ABSTRACT

In this paper, we carried out a laboratory experiment to study changes in canopy reflectance of Tamarugo plants under controlled water stress. Tamarugo (*Prosopis tamarugo* Phil.) is an endemic and endangered tree species adapted to the hyper-arid conditions of the Atacama Desert, Northern Chile. Observed variation in reflectance during the day (due to leaf movements) as well as changes over the experimental period (due to water stress) were successfully modelled by using the Soil-Leaf-Canopy (SLC) radiative transfer model. Empirical canopy reflectance changes were mostly explained by the parameters leaf area index (LAI), leaf inclination distribution function (LIDF) and equivalent water thickness (EWT) as shown by the SLC simulations. Diurnal leaf movements observed in Tamarugo plants (as adaptation to decrease direct solar irradiation at the hottest time of the day) had an important effect on canopy reflectance and were explained by the LIDF parameter. The results suggest that remote sensing based assessment of this desert tree should consider LAI and canopy water content (CWC) as water stress indicators. Consequently, we tested fifteen different vegetation indices and spectral absorption features proposed in literature for detecting changes of LAI and CWC, considering the effect of LIDF variations. A sensitivity analysis was carried out using SLC simulations with a broad range of LAI, LIDF and EWT values. The Water Index was the most sensitive remote sensing feature for estimating CWC for values less than 0.036 g/cm^2, while the area under the curve for the spectral range 910–1070 nm was most sensitive for values higher than 0.036 g/cm^2. The red-edge chlorophyll index ($CI_{red\text{-}edge}$) performed the best for estimating LAI. Diurnal leaf movements had an effect on all remote sensing features tested, particularly on those for detecting changes in CWC.

1. Introduction

Remote sensing (RS) has become an important tool to quantitatively assess and monitor water stress of vegetation, a key input for water management in arid regions. Water stress in plants activates a series of physiological mechanisms to maintain the water balance of the plant and to keep its vital functions, such as photosynthesis and respiration, while dehydrating (Taiz and Zeiger, 2010). Early stages of water stress are often related to loss of foliage water while late stages are related to loss in leaf pigments, loss of biomass (leaves, branches) and finally plants die (Baret et al., 2007; Taiz and Zeiger, 2010). These changes modify the light reflection and absorption properties of the vegetation canopy, which can be accurately registered by multispectral and hyperspectral instruments (Karnieli and Dall'Olmo, 2003).

Primary effects of water stress (dehydration) on vegetation spectral reflectance are associated with an increment of reflected radiation in the range of 1300–2500 nm solely because of less absorption by water (Carter, 1991; Zarco-Tejada et al., 2003). Secondary effects are associated with an increment of spectral reflectance in the range 400–1300 nm due to more cell wall–air interfaces within the leaf tissue as well as the effect of dehydration on the absorption properties of pigments (Carter, 1991; Knipling, 1970). Another secondary effect of water stress is the "blue shift" of the red edge (the steep slope of the vegetation spectral signature occurring at 680–750 nm) towards shorter wavelengths (Boochs et al., 1990; Carter, 1993; Filella and Penuelas, 1994; Horler et al., 1983). Although the spectral reflectance in the NIR region (700–1300 nm) initially increases (Clevers et al., 2010; Hunt and Rock, 1989), in late stages of water stress it decreases as a consequence of the deterioration of cell walls (Knipling, 1970) and loss of leaves (Asner, 1998). Furthermore, use of narrow spectral bands has

* Corresponding author. Tel.: +31 317 481552; fax: +31 317 419000.
E-mail addresses: roberto.chavez@wur.nl, roberto.chavez.o@gmail.com (R.O. Chávez).

0303-2434/$ – see front matter © 2012 Elsevier B.V. All rights reserved.
http://dx.doi.org/10.1016/j.jag.2012.08.013

enabled the identification of small spectral features also associated to water stress such as the right slope of the vegetation absorption feature at 970 nm (Clevers et al., 2010, 2008) related to canopy water content or the tiny jump in reflectance around 760 nm due to chlorophyll fluorescence (Pérez-Priego et al., 2005), which is a good indicator of stomatal conductance, CO_2 assimilation (Flexas et al., 2000, 2002) and water potential (Pérez-Priego et al., 2005). For a detailed summary of the sensitivity of different spectral regions to water stress and to other stress factors refer to Baret et al. (2007), Carter and Knapp (2001) and Govender et al. (2009).

Based on this knowledge, a considerable number of remote sensing based algorithms have been designed and implemented to quantitatively estimate and map important parameters related to plant water condition, such as leaf area index (LAI), leaf chlorophyll concentration and equivalent water thickness (EWT) (see Section 2.6).

Nevertheless, the application of remote sensing for assessing water condition of vegetation in hyper-arid ecosystems or "true deserts" is mainly conditioned by (i) the rather small size of the target objects (isolated trees, shrubs or grass patches), (ii) the knowledge on the response of desert species to water stress and potential effects on canopy spectral reflectance that are commonly unknown, and (iii) the species phenological cycles which have an important effect on the proportion of green and brown vegetation material during the year (Asner et al., 2000).

The low vegetation fractional cover and small size of vegetation units in deserts causes a high proportion of mixed pixels in most of the available RS datasets (i.e. Landsat, MODIS, SPOT, MERIS, RapidEye) (Asner and Heidebrecht, 2002). Recent improvements in spatial resolution of satellites such as Quickbird2, WorldView2 and GeoEye make it possible to obtain "comparatively pure" pixels of desert small trees and shrubs for more focused analysis on vegetation properties. Spectral resolution has also improved from the four standard bands of sub-metric satellites to up to eight bands in the visible and near infrared regions of WorldView2. All these improvements open new possibilities for remote sensing studies of desert vegetation, but also a need for better understanding of the canopy spectral properties of desert species.

Assessing water stress of vegetation adapted to hyper-arid conditions is not a straightforward process. Desert plant species have developed different mechanisms to tolerate dry conditions, either by controlling water content (via regulation of transpiration rates) or by drying up (partially or completely) and remaining latent until water supply conditions are again favourable (Alpert and Oliver, 2002). Therefore their natural dynamics and responses to external disturbances can significantly vary between different species and sites. These adaptations can radically influence vegetation canopy reflectance and absorption properties, and therefore a good understanding of this interaction is crucial for a reliable remote sensing based assessment.

In this study we aim to improve our understanding of the spectral response of the desert species *Prosopis tamarugo* Phil to water stress. Tamarugo is an endemic tree species, highly adapted to the hyper-arid conditions of the Atacama Desert, Northern Chile. Its geographic distribution is limited to the Atacama Desert and the trees are completely dependent on ground water (Altamirano, 2006; Mooney et al., 1980). Although most of the Tamarugo population is under official protection, the species is under threat due to ground water extraction for human consumption and mining (Rojas and Dassargues, 2007), and therefore, quantitative tools for assessing the forest water condition are needed for environmental policy making and monitoring.

Tamarugo tree response to water stress and the use of remote sensing to monitor this process has not been studied. In order to provide basic knowledge for a remote sensing based assessment of Tamarugo, we conducted a laboratory experiment to study the response of Tamarugo plants to controlled water stress. Specifically, through this experiment we aim to (1) describe the physiological and spectral response of Tamarugo plants to water stress, (2) define appropriate canopy variables for assessing water stress for this species, (3) model the spectral response of a Tamarugo canopy to water stress using the radiative transfer theory and (4) test the sensitivity of different indices and spectral features to detect water stress using a range of simulated scenarios.

2. Materials and methods

2.1. Species description

Tamarugo (*P. tamarugo* Phil.) is a xerofitic tree species highly adapted to the extreme arid conditions of the Atacama Desert, Northern Chile (Fig. 1). This hyper-arid environment is characterized by practically null precipitation, high temperatures and high potential evapotranspiration (Houston, 2006; Houston and Hartley, 2003) and it is considered one of the most extreme environments for life on Earth (McKay et al., 2003; Navarro-González et al., 2003). The presence of Tamarugo is explained by the existence of a shallow groundwater table (Mooney et al., 1980), occurring in just two hydrological systems: Pampa del Tamarugal aquifer and Llamara aquifer, where practically all remaining Tamarugo population is distributed. Studies have shown that natural and artificial (pumping) discharges in the Pampa del Tamarugal aquifer have been twice as large as natural recharges since 1986 (Rojas and Dassargues, 2007). Consequently, groundwater gradually has depleted threatening Tamarugo water supply. Between 1965 and 1970 a big effort for Tamarugo's conservation was promoted by the Chilean government and around 13,800 ha were planted (Aguirre and Wrann, 1985; CONAF, 1997).

Tamarugos are thorny phreatophyc trees and reach heights up to 25 m, crown size up to 20 m and stems up to 2 m in diameter (Altamirano, 2006; Riedemann et al., 2006). Tamarugo is a semicaducifolious tree, keeping a considerable part of its foliage during the winter (Sudzuki, 1985). Its vegetative period covers all year with a peak occurring between September and December (Acevedo et al., 2007). The branches are arched and gnarled, twigs are flexuose and thorns in pairs are stipular in origin of 0.5–3.8 cm (Trobok, 1985). Leaves are often bipinnate with 6–15 pairs of folioles (Fig. 1b and c).

2.2. Experimental setup

A total of nine plants, about 30 cm in height, were placed in a climate chamber with no water supply for 15 days. Plants were grown under greenhouse conditions and kept in the original black containers and substrate during the whole experiment. The plants were arranged in a matrix of 3×3 in such a way that a continuous canopy (including leaves, stems and soil) was available for nadir spectral measurements. The climate chamber was deprived of sunlight and artificial light was provided by an ASD Pro lamp. This is a 14.5 V 50 W lamp especially designed for laboratory diffuse reflectance measurements over the region 400–2500 nm. The applied light regimen consisted of 14 h light from 7:00 h till 21:00 h followed by 10 h of darkness and the temperature was set at 30 °C (±5 °C), similar to Tamarugo's natural conditions during summer (Houston, 2006; Mooney et al., 1980). A spectroradiometer instrument (ASD FieldSpec Pro) was installed above the plants in order to measure spectral reflectance in the range 400–2500 nm. A foreoptic with instantaneous field of view (IFOV) of 25° was used and placed in nadir position 15 cm above the top of the canopy. This setup gave a circular measurement area of green plants of approximately 35 cm^2. No laboratory background was within the IFOV of the ASD instrument.

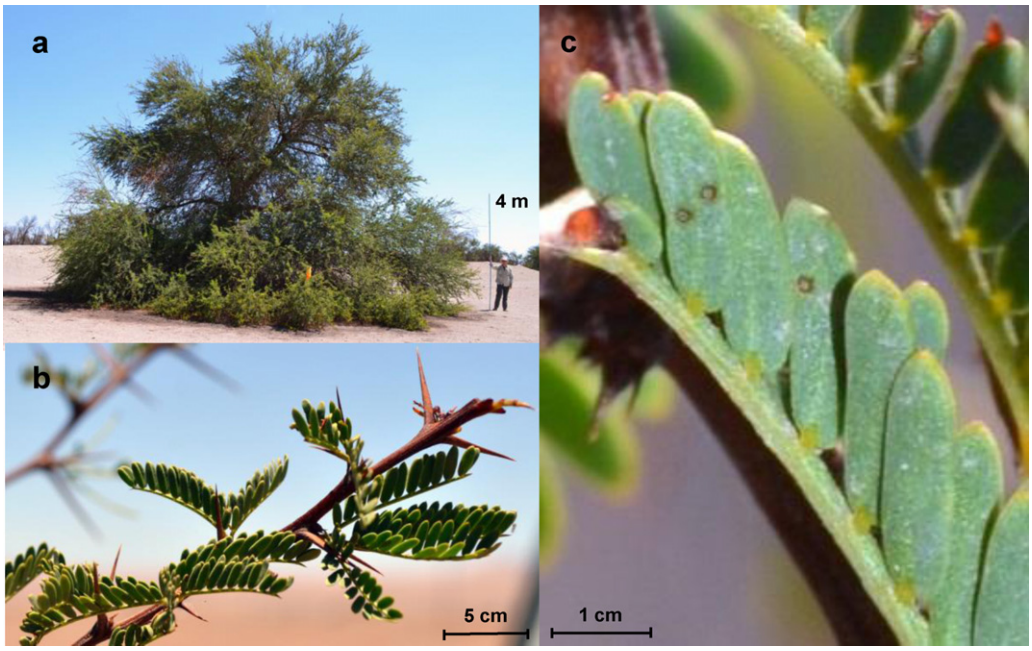

Fig. 1. Anatomic characteristics of *Prosopis tamarugo* Phil. (a) Adult tree; (b) Twig; and (c) composed bipinnate leaf.

2.3. Spectral sampling

Spectral sampling was performed hourly, starting at 8:00 h and ending at 20:00 h (13 samples per day), in order to study the course of spectral reflectance during the day. This was repeated for 14 days in order to investigate the spectral response to water stress. The last spectral sampling was done on day 15 at 8:00 h. Each sample corresponded to a spectral signature in the range 400–2500 nm obtained as an average of 50 scans. White reference measurements (spectralon) were used to obtain bi-conical reflectance factor measurements according to the nomenclature proposed by Schaepman-Strub et al. (2006). White reference calibrations were carried out at the beginning of the experiment as well as on day 5 and day 10. Previous tests showed a good stability of the ASD measurements within the chamber, so calibrations were minimized to avoid disturbing the experiment.

2.4. Physiological sampling

Physiological sampling was carried out daily at 8:30 h during 15 days. The physiological measurements included equivalent water thickness (EWT) in g/cm^2, leaf chlorophyll concentration (*a*, *b* and total) in μg/cm^2 and leaf carotenoids concentration in μg/cm^2. Leaves from the lower third of the plants were used for laboratory determinations. No leaf sampling was carried out within the IFOV of the ASD instrument.

Leaf samples for chlorophyll and carotenoid determinations were spectro-photometrically analysed using leaf extracts dissolved in 80% acetone. Absorbance measured at 663 nm was utilised to determine chlorophyll *a*, at 646 nm for chlorophyll *b* and at 479 nm for carotenoids.

Equivalent water thickness (EWT) was measured using the following formula:

$$\text{EWT} = \frac{(\text{fresh leaf weight} - \text{dry leaf weight})}{\text{fresh leaf area}} \quad (1)$$

The fresh weight was measured immediately after cutting the leaves using a digital balance of 0.0001 g precision. Dry weight was obtained by drying the samples in an oven at 75 °C until getting constant dry weight.

2.5. Spectral absorption feature analysis

Continuum removal is a useful spectral processing methodology for studying the relationship between spectral absorption features and the biochemical composition and water content of a vegetation canopy (Huang et al., 2004; Huber et al., 2008; Kokaly and Clark, 1999), which both are indicators of water stress. Furthermore, continuum removal minimizes the undesired effects of soil background and atmospheric absorptions on the spectral analysis (Kokaly and Clark, 1999). Features of interest in spectral absorption feature analysis are the maximum band depth (MBD), the area under the curve (AUC) and the MBD normalized by the AUC (MBD/AUC) (Curran et al., 2001). An example of continuum removal applied to the canopy spectral signature of Tamarugo is given in Fig. 2. Typically, the chlorophyll absorption feature in the visible part of the spectrum has been described as occurring approximately between 550 and 750 nm (Curran, 1989; Huber et al., 2008; Kokaly et al., 2003). Furthermore, there are two absorption features associated with the presence of water in plant foliage: the first around 970 nm and the second one around 1200 nm (Curran, 1989). There are also water absorption features at 1400 and 1900 nm, but they are not of interest for remote sensing applications since they are strongly affected by atmospheric water vapour (Clevers et al., 2008).

In this study continuum removal was applied to analyse changes in the chlorophyll absorption feature (at 670 nm) and water absorption features (at 970 and 1200 nm) due to water stress. Spectral signatures measured daily at 8:00 h during the 15 days of the laboratory experiment were used.

2.6. Remote sensing features for assessing water stress

In this study we explore the sensitivity of different RS based approaches to detect water stress in Tamarugos. Empirical models as well as physical models have been used to remotely retrieve LAI, chlorophyll concentration and EWT, main symptoms of plant stress (Baret et al., 2007). Radiative transfer models use physical laws to describe the interaction between light, the vegetation canopy and background (Jacquemoud et al., 2009). They establish an

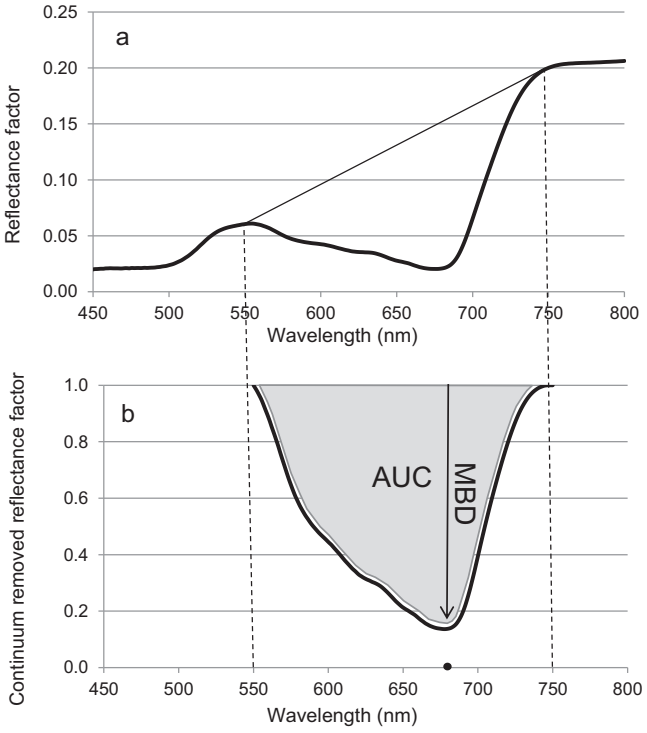

Fig. 2. Example of continuum removal applied to a Tamarugo spectral signature. (a) Original spectrum and (b) continuum removed spectrum.

explicit linkage between the canopy reflectance and biochemical and structural properties of the scattering elements of vegetation. Radiative transfer models can be used in the "forward" way to simulate different scenarios of canopy reflectance when vegetation properties vary (this study). They can also be used in the "inverse" way (from canopy reflectance to vegetation properties) to estimate vegetation parameters from remotely sensed or ground measured canopy reflectance (Colombo et al., 2008; Jacquemoud et al., 2009; Laurent et al., 2011a; Vohland et al., 2010; Zarco-Tejada et al., 2003). This inversion process can be complex due to the large amount of parameters involved in the models and therefore the use of prior information or constraints is necessary for a successful estimation (Combal et al., 2003).

Empirical models establish statistical relationships between specific reflectance features of the vegetation spectra and vegetation parameters. Widely used empirical models are the so-called vegetation indices (VIs) which combine a limited amount of spectral information through a numerical indicator that is statistically correlated with specific vegetation parameters. Examples of indices to assess loss in LAI are the Ratio Vegetation Index (RVI) (Jordan, 1969), the widely used Normalized Difference Vegetation Index (NDVI) (Tucker, 1979) and the Wide Dynamic Range Vegetation Index (WDRVI) (Gitelson, 2004). The sharp slope of the vegetation spectral signature occurring at 680–750 nm, the red-edge, has been described to be very sensitive to changes in LAI and leaf chlorophyll (Boochs et al., 1990; Filella and Penuelas, 1994) and the Red Edge Position (REP) has been used to retrieve LAI with even better results than using NDVI (Danson and Plummer, 1995; Herrmann et al., 2011). Furthermore, VIs like the red-edge Chlorophyll Index ($CI_{red\text{-}edge}$) and red-edge Normalized Difference Vegetation Index (red-edge NDVI) have been developed to retrieve specifically leaf chlorophyll content (Gitelson and Merzlyak, 1994; Gitelson et al., 2006), but they also have been utilised for retrieving LAI (Viña et al., 2011). For assessing water stress in terms of EWT or canopy water content (CWC = EWT × LAI), VIs like the Water Index (WI) (Peñuelas et al., 1997), the Normalized Difference Water Index (NDWI) (Gao, 1996) and more recently the derivative [1015–1050 nm] (Clevers et al., 2010) can be used. These indices are based on the water absorption features at 970 nm and 1200 nm and use specific narrow bands.

In this study, the spectral and physiological changes observed during the experiment (Sections 3.1 and 3.2) as well as the spectral absorption feature analysis (Section 3.3) were used as a base for identifying suitable canopy variables and remote sensing methods to assess water stress of Tamarugo (Table 1). A sensitivity analysis was carried out by using a broad range of simulated scenarios using the radiative transfer model Soil-Leaf-Canopy (see Section 2.7) and the noise equivalent (NE) statistic as sensitivity indicator (see Section 2.8).

2.7. SLC model calibration and simulations

The Soil-Leaf-Canopy (SLC) model (Verhoef and Bach, 2007) simulates top of canopy reflectance using as inputs leaf, canopy and soil parameters (Table 2).

The SLC version used in this study is the result of coupling the following models:

- *PROSPECT3* (Jacquemoud and Baret, 1990) was modified to include the effects of brown pigments (Verhoef and Bach, 2003) and it delivers simulations at 10 nm spectral resolution.
- *4SAIL2* (Verhoef and Bach, 2007) is an improved version of the canopy radiative transfer model SAIL (Verhoef, 1984). Among the new features, this 2-layer version includes the effects of crown clumping and the effects of the abundance and distribution of green and brown elements within the two canopy layers (Verhoef and Bach, 2007), which allows a more realistic representation of the canopy and thus gives improved simulations.
- *SOIL4* (Hapke, 1981; Verhoef and Bach, 2007) includes the hotspot effect and the soil moisture spectral effect. In this study a measured background was used for calibrations and simulations, and therefore soil reflectance was fixed.

Physiological and spectral measurements carried out on day 1 at 8:00 h were used to calibrate the SLC model. The parameters LAI, LIDFa, and LIDFb (Table 2) were optimized by minimizing the differences between measured and simulated reflectance values. In this optimization procedure, the parameters measured at the laboratory (Cab_{green}, EWT_{green}, and Cdm_{green}) were considered fixed. For the other parameters the default values of the SLC model were used as indicated in Table 2. The parameters of the 4SAIL2 second layer (brown elements, i.e. stems and twigs) were optimized using the spectral reflectance measured at the end of the experiment, when no green leaves were present. A similar methodology often has been used for assessing radiative transfer model simulations using measured spectra; examples can be found in Darvishzadeh et al. (2011) and Laurent et al. (2011a,b).

Once calibrated, the SLC model was used to simulate spectral reflectance for a wide range of water stress scenarios. These outputs were used to test the sensitivity of RS features indicated in Table 1.

2.8. Sensitivity of remote sensing features for assessing water stress

For the sensitivity analysis a total of 528 simulations were carried out by varying the equivalent water thickness (EWT), leaf area index (LAI) and the parameter *a* (slope parameter) of the leaf inclination distribution function (LIDF) as shown in Table 3. The whole range of observed water stress conditions was simulated. LAI values ranging from 0 to 2 were used for the simulations considering LAI measurements made by the authors in the field.

Table 1
Remote sensing features tested for assessing water stress of Tamarugo plants in terms of LAI and CWC.

Remote sensing feature	Formula and spectral regions used in this study	References
For assessing CWC		
Water Index (WI)	R_{900}/R_{970}	Peñuelas et al. (1997)
Normalized Difference Water Index (NDWI)	$(R_{860}-R_{1240})/(R_{860}+R_{1240})$	Gao (1996)
Derivative [1015, 1050]	$(R_{1015}-R_{1050})/35$	Clevers et al. (2010)
Water absorption feature [910–1070 nm]		Clark and Roush (1984)
MBD		
AUC		
MBD/AUC		
Water absorption feature [1100–1280 nm]		Clark and Roush (1984)
MBD		
AUC		
MBD/AUC		
For assessing LAI		
Normalized Difference Vegetation Index (NDVI)	$(R_{800}-R_{670})/(R_{800}+R_{670})$	Tucker (1979)
Red-edge Chlorophyll Index ($CI_{Red\text{-}edge}$)	$R_{780}/R_{710}-1$	Gitelson et al. (2006)
Red-edge NDVI	$(R_{780}-R_{710})/(R_{780}+R_{710})$	Gitelson and Merzlyak (1994)
Ratio Vegetation Index (RVI)	R_{800}/R_{670}	Jordan (1969)
Chlorophyll absorption feature [550–750 nm]		Clark and Roush (1984)
MBD		
AUC		

MBD, maximum band depth; AUC, area under the curve.

Using this simulated dataset, the relationship between the RS features and CWC or LAI was analysed by using the best-fit functions. CWC was calculated as follow:

$$\mathrm{CWC} = \mathrm{EWT} \times \mathrm{LAI} \quad (2)$$

In order to compare the different RS features, which present different scales and dynamic ranges, the absolute value of the Noise Equivalent (NE) ΔCWC and NEΔLAI were used (Viña and Gitelson, 2005).

$$\mathrm{NE}\Delta\mathrm{CWC} = \frac{\mathrm{RMSE}\{\mathrm{RSfeature\ vs.\ CWC}\}}{\mathrm{Abs}\{d(\mathrm{RSfeature})/d(\mathrm{CWC})\}} \quad (3)$$

$$\mathrm{NE}\Delta\mathrm{LAI} = \frac{\mathrm{RMSE}\{\mathrm{RSfeature\ vs.\ LAI}\}}{\mathrm{Abs}\{d(\mathrm{RSfeature})/d(\mathrm{LAI})\}} \quad (4)$$

Table 2
Soil-Leaf-Canopy (SLC) model input parameters.

SLC inputs		Day 1 – 8.00	Day 1 – 20.00	Day 14 – 8.00	Day 14 – 20.00	Source
Leaves (green material)						
Chlorophyll ab content (μg/cm)	Cab_{green}	42	42	42	42	Lab. measurement
Water content (g/cm^2)	**EWT_{green}**	**0.023**	**0.023**	**0.013**	**0.013**	**Lab. measurement**
Dry matter content (g/cm^2)	Cdm_{green}	0.0003	0.0003	0.0003	0.0003	Lab. measurement
Senescent material (no units)	Cs_{green}	0	0	0	0	From experiment
Mesophyll structure (no units)	N_{green}	1.5	1.5	1.5	1.5	SLC default
Twigs and stems (brown material)						
Chlorophyll ab content (μg/cm)	Cab_{brown}	5	5	5	5	SLC default
Water content (g/cm^2)	EWT_{brown}	0.01	0.01	0.01	0.01	Optimized
Dry matter content (g/cm^2)	Cdm_{brown}	0.005	0.005	0.005	0.005	SLC default
Senescent material (no units)	Cs_{brown}	1	1	1	1	SLC default
Mesophyll structure (no units)	N_{brown}	2	2	2	2	SLC default
Canopy						
Plant area index[a] (m^2/m^2)	PAI	1.27	1.27	1.12	1.12	Optimized
Leaf area index (m^2/m^2)	**LAI**	**1.00**	**1.00**	**0.85**	**0.85**	**Optimized**
Brown area index (m^2/m^2)	BAI	0.27	0.27	0.27	0.27	Optimized
Leaf inclination distribution function a[b] [−1, +1]	**LIDF a**	**−0.30**	**−0.45**	**0.10**	**0.02**	**Optimized**
Leaf inclination distribution function b[c] [−1, +1]	LIDF b	−0.15	−0.15	−0.15	−0.15	SLC default
Hot spot effect parameter[d]	Hot	0.05	0.05	0.05	0.05	SLC default
Fraction brown PAI [0,1]	fb	0.21	0.21	0.24	0.24	Optimized
Dissociation factor [0,1]	D	0.8	0.8	0.8	0.8	SLC default
Vertical crown coverage [0,1]	Cv%	100	100	100	100	From experiment
Tree shape factor[e]	Zeta	0.5	0.5	0.5	0.5	From experiment
Solar zenith angle (degrees)	sza	30	30	30	30	From experiment
Viewing zenith angle (degrees)	vza	0	0	0	0	From experiment
Sun-view azimuth difference (degrees)	azi	0	0	0	0	From experiment
Soil						
Soil background		Measured values	Measured values	Measured values	Measured values	Lab. measurement

[a] PAI = LAI + BAI. PAI and fb change because LAI change.
[b] Leaf slope indicator.
[c] Bimodality parameter.
[d] Estimated as the ratio of the average leaf width and the canopy height.
[e] Diameter/height.

Table 3
Soil-Leaf-Canopy (SLC) parameter range and intervals used for simulations.

SLC parameters	Min	Max	Step	# Values
Cw_{green}	0.005	0.03	0.005	6
LAI	0	2	0.20	11
LIDF*a*	−0.50	0.20	0.10	8

where RMSE is the root mean squared error of the best-fit function of the relationship between the RS feature and LAI or CWC, respectively, and d(RSfeature)/d(CWC) and d(RSfeature)/d(LAI) are the corresponding first derivatives of the best-fit functions. Small values for NEΔCWC and NEΔLAI indicate strong sensitivity for CWC and LAI, respectively.

3. Results

3.1. Physiological response of Tamarugo plants under water stress

The results of the physiological sampling in terms of equivalent water thickness, leaf chlorophyll and leaf carotenoid concentration are depicted in Fig. 3.

No evident symptoms of stress were observed in the leaf samples until day 11 when the EWT started to drop from values of 0.025 g/cm^2 down to values of 0.005 g/cm^2 on day 15 (Fig. 3a). Average EWT during the first ten days was 0.023 g/cm^2. There was not a clear trend in the observed values of leaf chlorophyll concentration and carotenoid concentration. During the experiment, it was observed that the plants were gradually drying some leaves while keeping the remaining leaves healthy. From day 10 onwards the amount of dry leaves increased rapidly. However, due to the absence of natural disturbances (like wind) most of the dry leaves remained on the twigs. At day 15 there were few remaining green leaves.

Average values of leaf chlorophyll concentrations for the whole period were 15.9 μg/cm^2 for chlorophyll *a*, 26.0 μg/cm^2 for chlorophyll *b* and 42 μg/cm^2 for total chlorophyll. Leaf carotenoid concentration was rather constant with an average value of 1529 μg/cm^2.

3.2. Spectral response of Tamarugo plants under water stress

3.2.1. Changes in diurnal reflectance

In the absence of water stress, it was observed that plants modified the incidence angle of light on the leaves by changing the orientation of the folioles (Fig. 4). As a matter of fact, the orientation of the folioles changed towards a more erectophile leaf distribution (parallel to incoming light rays) after midday. This means leaves avoided to face direct irradiation past noon.

Consequently, reflectance decreased from midday onwards (Fig. 5a). Changes occurred despite the angle of illumination (ASD lamp) was fixed at 30° from nadir. Observations made on Tamarugo leaves suggest the presence of a pulvinus, a thickening in the leaf base, which often is the structure responsible for leaf movements (Fig. 1c). Pulvinar movements have been described for other species with composed leaves (Barchuk and Valiente-Banuet, 2006; Ezcurra et al., 1992; Liu et al., 2007) and they are associated with contraction–expansion mechanisms driven by cell turgor changes (Taiz and Zeiger, 2010). Therefore, Tamarugo leaf movement can be affected by water stress. Under water stress, leaf cells may have run out of water and, as a consequence, folioles were less able to change the leaf angle. Hence, reflection became more constant throughout the day and the difference between morning and afternoon became smaller (Fig. 5b and c). The ability of Tamarugo plants to adjust the leaf angle is a good example of how some adaptations of desert species can influence reflectance properties. For this reason, remote sensing approaches should take into account the biology of arid species to accurately assess the water condition of vegetation in arid environments. More insight is needed to understand the influence of leaf movement of the Tamarugo plant on canopy reflectance under natural conditions, where the incoming solar irradiation is changing (position and intensity) throughout the day. This will be subject for further research.

3.2.2. Reflectance changes over the experimental period

Besides the morning–evening changes in spectral reflectance, more changes can be observed when comparing the spectra of days 1–3 (Fig. 5b, no stress) with, e.g., days 12–14 (Fig. 5c, under stress). Reflectance over the infrared region increased as a consequence of the dehydration process. This is due to the larger number of cell wall–air interfaces within the leaf tissue, caused by the absence of water, which produces an increment of internal multiple reflections of NIR radiation (Carter, 1991; Knipling, 1970).

Furthermore, the water absorption at 1400 and 1900 nm decreased, which is a clear indication of the dehydration process (Carter, 1991; Hunt and Rock, 1989). The water absorption features at 970 and 1200 nm were too small for visual inspection and for this reason continual removal was applied to quantitatively study changes due to water stress (Section 3.3).

Despite senescence, leaves hardly fell during the experiment because within the climate chamber there were no natural disturbances such as wind and decrease in LAI was limited. After measuring spectral and physiological variables on day 15 at 8:00 h, plants were shaken and dry leaves immediately fell down. Then the spectral reflectance was measured. Subsequently, all green leaves were cut off and the spectral signature was measured again. This way the effects of losing dry and green leaves on spectral reflectance were registered as shown in Fig. 5d.

3.3. Chlorophyll and water absorption features

The continuum removal analysis carried out for the *chlorophyll absorption feature* showed that both MBD and AUC were progressively decreasing over the days (Fig. 6a and b), while the ratio MBD/AUC was slightly increasing in time (Fig. 6c). These results differ from the chlorophyll measurements for single leaves (Fig. 3), which showed slight differences of chlorophyll concentration over time. Therefore, it can be inferred that changes in the chlorophyll absorption feature are due to LAI decrease rather than degradation or relocation of leaf chlorophyll. This is in line with the SLC simulations performed and described in Section 3.4. The fact that the MBD decreased in time suggests that ratio vegetation indices using the NIR spectral region (760–900 nm) and the red (630–690 nm) or the NIR and the red-edge region (680–750 nm) can be used for assessing water stress in terms of LAI loss. MBD, AUC and MBD/AUC also can be used for estimating changes in LAI.

Water absorption features of healthy Tamarugo plants occurred at 973 nm and 1165 nm. MBD, AUC and MBD/AUC of both absorption features decreased over the days, showing a linear trend (Fig. 6). This differs from the trend observed for EWT measurements for single leaves (Fig. 3a), where the effects of water stress were observed from day 11 onwards, and could be explained by the fact that the ASD instrument is measuring a surface of stacked leaves rather than single leaves. Therefore, the measured spectral signature is an integrative measure of the water status of the complete canopy within the ASD IFOV. For this reason, the variable canopy water content (CWC) defined as the product between LAI and EWT is often used in vegetation studies.

These results suggest that ratio vegetation indices using the spectral regions where the water absorption features occur, such as WI and NDWI, can be used for estimating changes in CWC (Table 1). Another interesting feature is the change on the right slope of the

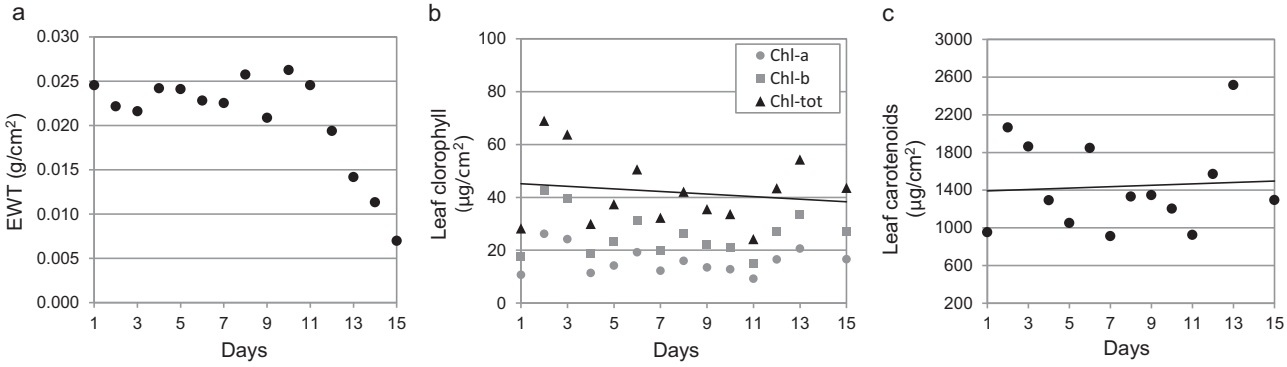

Fig. 3. Physiological parameters measured during the experiment. (a) Equivalent water thickness, (b) leaf chlorophyll concentration and (c) leaf carotenoids concentration.

absorption feature at 973 nm, which recently has been proposed and tested as a good indicator of canopy water content (Clevers et al., 2010, 2008).

3.4. SLC calibration and simulations

The calibration of the SLC model was performed using the spectral values measured on day 1 at 8:00 h and physiological values measured during the experiment. The correspondence between simulated and measured spectra was good over the full spectral range (Fig. 7a) with an RMSE of 0.006 when comparing simulated and measured spectral reflectance.

Subsequently, the slope parameter of the leaf angle distribution function (LIDF*a*) was optimized to fit the measured spectrum at 20:00 h. This parameter controls the average leaf slope and ranges from −1 to 1 (Verhoef and Bach, 2007). Values of LIDF*a* close to 1 correspond to a planophile distribution, values close to 0 to a uniform (random) distribution and values close to −1 to an erectophile distribution (Verhoef and Bach, 2007). Results of the optimization procedure showed that the LIDF*a* parameter by itself explained the changes in reflectance observed during the day (Fig. 7a). Matching simulated reflectance curves were obtained by varying the LIDF*a* parameter from −0.30 at 8:00 h to −0.45 at 20:00 h. So, changing this parameter towards more negative values is reproducing the leaf movement observed during the experiment: leaves changing towards a more erectophile leaf distribution after midday (Fig. 4).

The SLC parameters LAI and LIDF*a* were then tuned to fit the measured reflectance spectrum of day 14 when the plants were under water stress (measured EWT value of 0.013 was used, see Table 2). Correspondence between simulated and measured spectra was good (Fig. 7b) with an RMSE of 0.008 for the spectral reflectance at 8:00 h and 0.009 for the spectral reflectance at 20:00 h. Once again, reflectance changes between morning and evening on day 14 were explained by the LIDF*a* parameter, while changes from day 1 to 14 were explained mainly by decreasing LAI and EWT (Table 2, bold values). This time LIDF*a* values for both morning and evening were close to zero (0.10 and 0.02), which corresponds to a more uniform distribution, resembling a canopy where leaf slope is randomly distributed. This change in LIDF can be interpreted as an effect of water stress on the pulvinar movement of Tamarugo plants, and consequently, on their ability to move the leaves over the day.

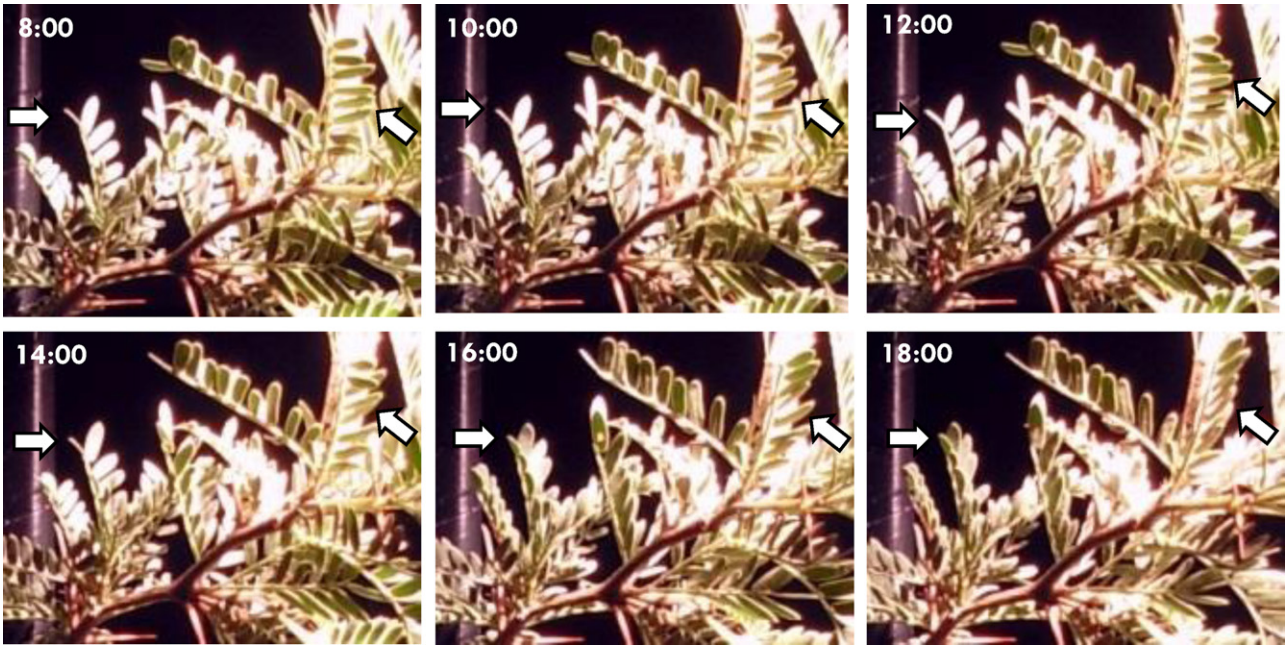

Fig. 4. Folioles orientation changing throughout day 1.

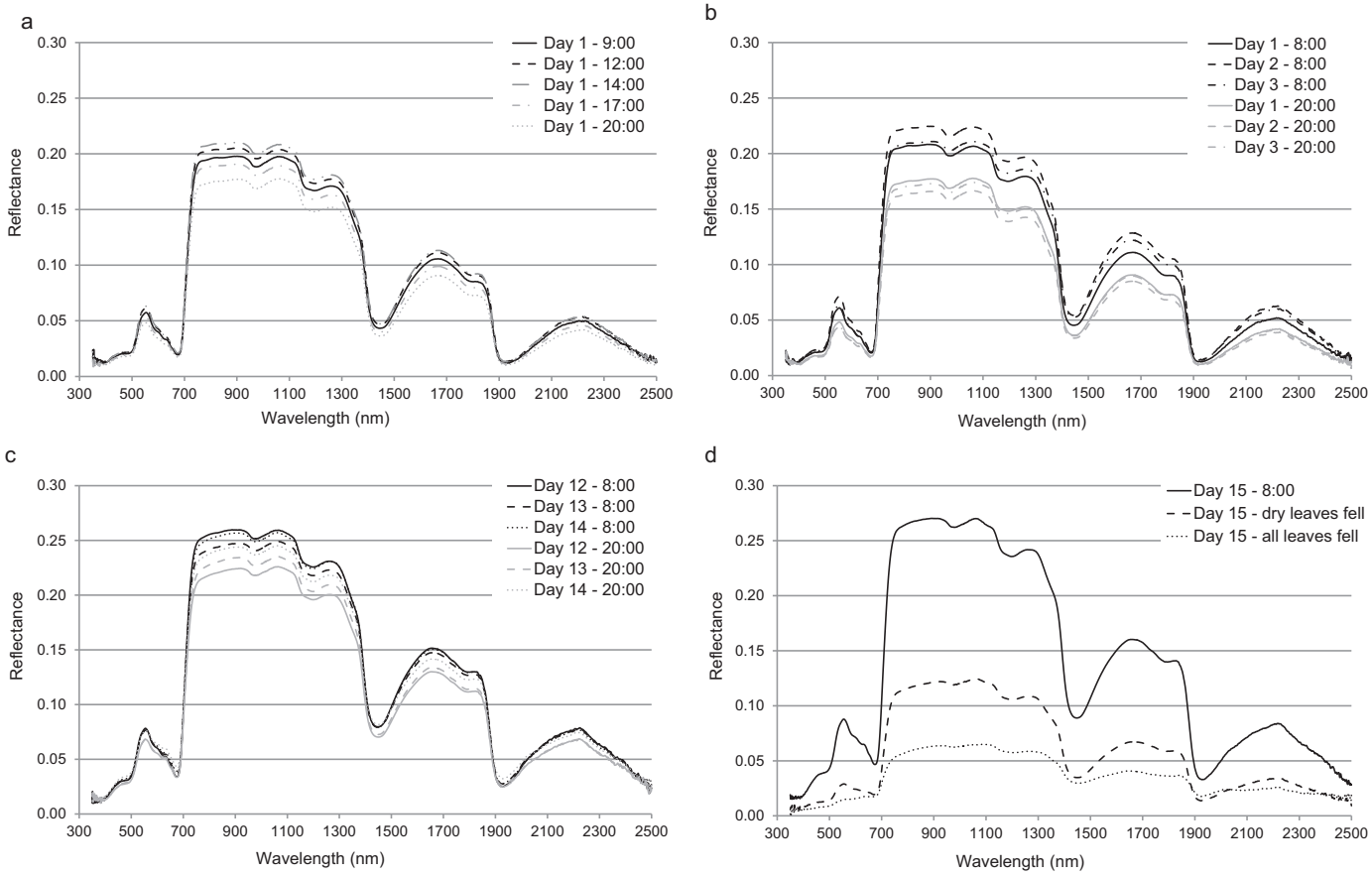

Fig. 5. Canopy spectral reflectance measured under laboratory conditions. (a) Diurnal changes from 9:00 to 20:00 h of day 1, (b) Morning–evening differences for days 1–3 (no water stress), (c) Morning–evening differences for days 12–14 (under water stress) and (d) changes due to defoliation.

3.5. Evaluation of remote sensing features for assessing water stress

3.5.1. Remote sensing features for detecting changes in canopy water content

Fig. 8 summarizes the relationship between nine remote sensing features analysed and canopy water content (CWC). The analysis showed an asymptotic relationship for all ratio RS features, i.e. WI, NDWI, MBD/AUC [910–1070] and MBD/AUC [1100–1280], which means they become less sensitive for high values of CWC. The derivative [1015–1050], MBD and AUC for both [910–1070 nm] and [1015–1050 nm] water absorption features showed a linear relationship, but different scatter around the fitted line. The derivative [1015–1050] showed the largest scatter, which is increasing concurrently with CWC values. Daily changes of leaf slope (LIDF*a*) observed for Tamarugo plants (Fig. 4) induced changes in the right slope of the water absorption feature at 970 nm affecting the prediction capability of this RS feature.

A comparison of the tested RS features for estimating changes in CWC was performed by means of the NEΔCWC (Eq. (3)). Low values of NEΔCWC indicate high sensitivity to changes in CWC. The sensitivity analysis (Fig. 9) showed that most of the indices lose sensitivity when CWC increases, especially the MBD/AUC [1100–1280]. The most sensitive RS feature for detecting changes in CWC was the WI for the CWC range from 0.01 to 0.036 g/cm^2. For estimating CWC values larger than 0.036 g/cm^2 the AUC [910–1070] was the most sensitive feature while for values lower than 0.01 the NDWI was the most sensitive.

3.5.2. Remote sensing features for detecting changes in leaf area index

Fig. 10 summarizes the relationship between six remote sensing features analysed and leaf area index (LAI). The indices NDVI, red-edge NDVI as well as the MBD [550–750] and AUC [550–750] showed an asymptotic relationship with LAI with high sensitivities for LAI values less than 1. In the case of RVI the relationship was linear; however, it exhibited increasing scatter for high LAI values. This can be explained by the error introduced by varying the LIDF*a* parameter in the SLC simulation, which is simulating the observed changes in the leaf slope. $CI_{red\text{-}edge}$ showed a relationship with LAI close to linear showing a high sensitivity to changes in LAI for the whole range.

Finally, a multiple comparison of all RS features is presented in Fig. 11 by means of the NEΔLAI. Except for the Ratio Vegetation Index (RVI), all the tested RS features were very sensitive (low NEΔLAI values) to changes in LAI in the range from 0 to 0.5. From this value onwards, the sensitivity of MBD [550–750], AUC [550–750] and NDVI decreased exponentially. The sensitivity of the RVI was constant over the whole LAI range, constituting a good predictor for LAI in the range from 1 to 2 and the most sensitive for values >1.6. Overall, the most sensitive RS feature considering the whole range of LAI values was the $CI_{red\text{-}edge}$.

4. Discussion and conclusions

This experiment showed that Tamarugo plants are able to adjust the leaf slope to avoid direct irradiation past noon, an adaptation

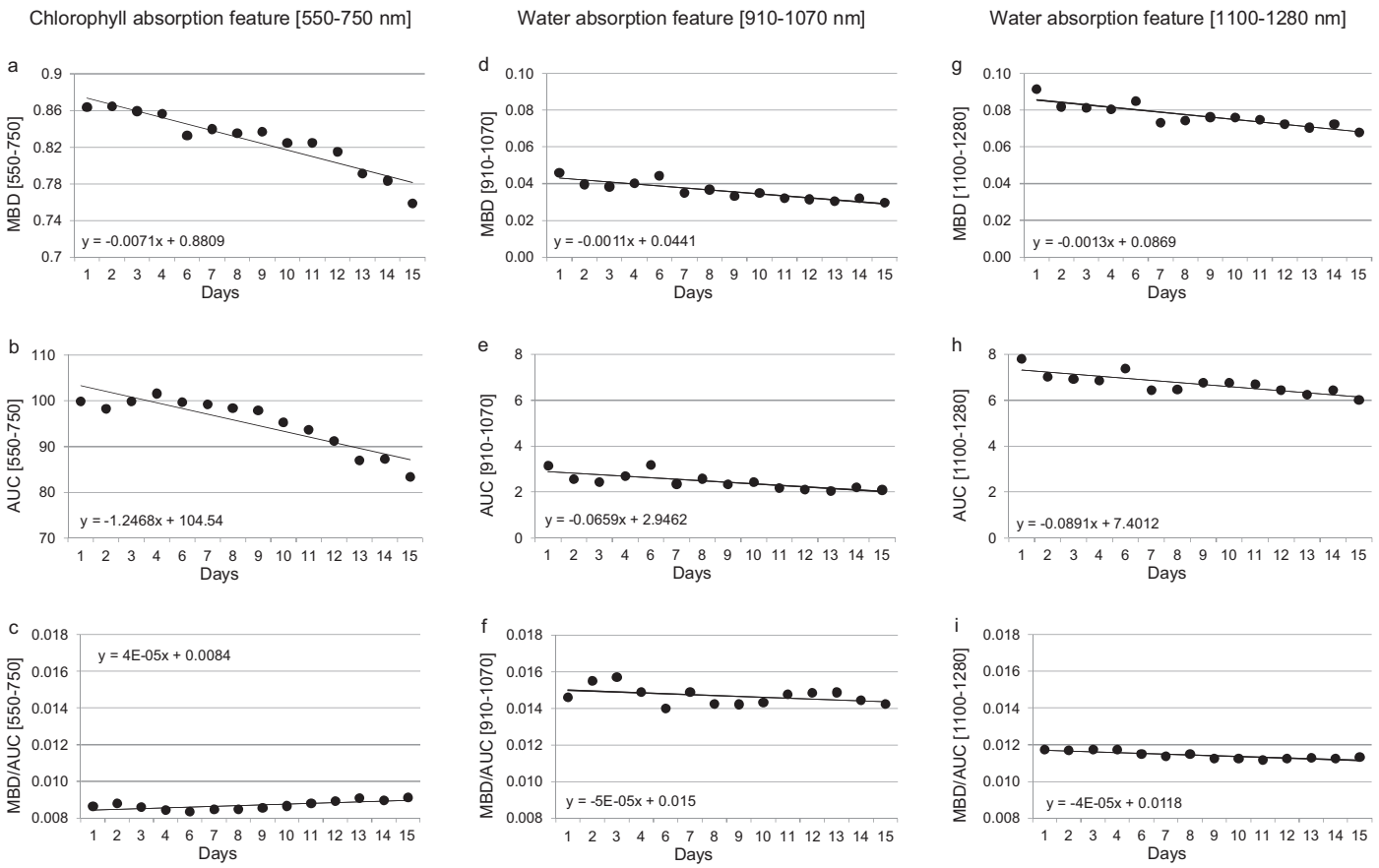

Fig. 6. Evolution of the chlorophyll [550–750 nm] and water absorption features [910–1070 nm], [1100–1280 nm] during the experimental period. Absorption features are shown in terms of maximum band depth (MBD), area under the curve (AUC) and the ratio MBD/AUC.

which has an important effect on the spectral reflectance over the whole 400–2500 nm range. This leaf movement, technically known as heliotropism or sun tracking (Raven et al., 2005), is most likely controlled by a pulvinar structure present on the folioles base of Tamarugo plants (Fig. 1c) and it is known as a common ability of the Leguminosae plants to avoid photoinhibition (Liu et al., 2007; Pastenes et al., 2004, 2005). Measurements done with an ASD spectroradiometer showed that daily canopy reflectance, under the non-stress scenario, decreased from midday onwards as a consequence of this leaf movement. This is likely to be a process controlled by changes in cell turgor of the pulvinus and therefore can be affected by water stress. Under water stress, leaves dehydrated and consequently folioles were not able to change the incidence angle of light on their leaves anymore. Therefore, reflection during the day became more constant and the difference between morning and afternoon smaller. From day 11 onwards, plants responded to water stress by drying out some leaves while keeping the remaining leaves green. When this occurred, dry leaves have a bigger chance to fall down (dehiscent). As a consequence of the resulting loss in water content, spectral reflectance increased over the whole spectrum and the chlorophyll absorption feature at 670 nm as well as the water absorption features at 970 nm and 1200 nm decreased.

Changes in reflectance during the day as well as changes along the experimental period were successfully modelled by using the

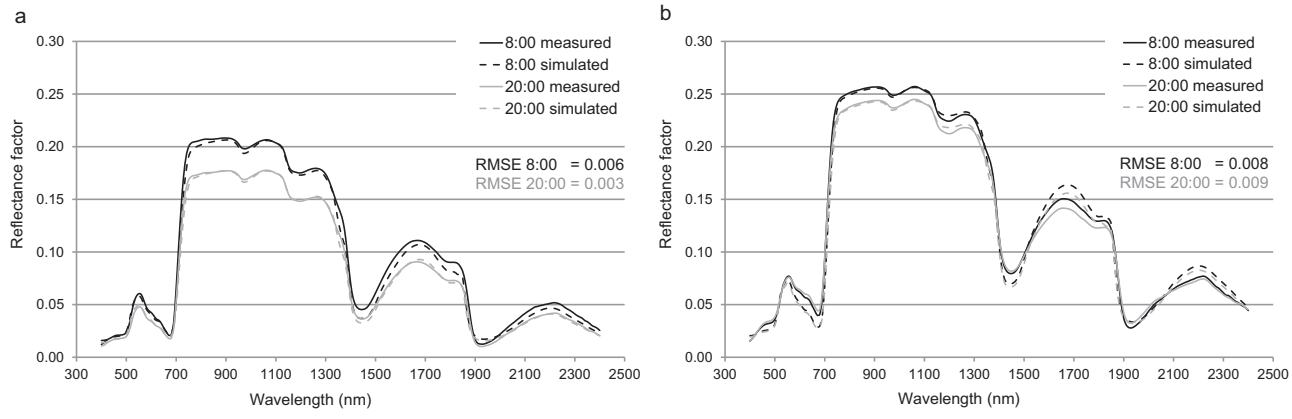

Fig. 7. Canopy spectral reflectance of a) day 1 (no water stress), and b) day 14 (under water stress). Continuous lines correspond to ASD measurements and dashed lines to SLC simulations.

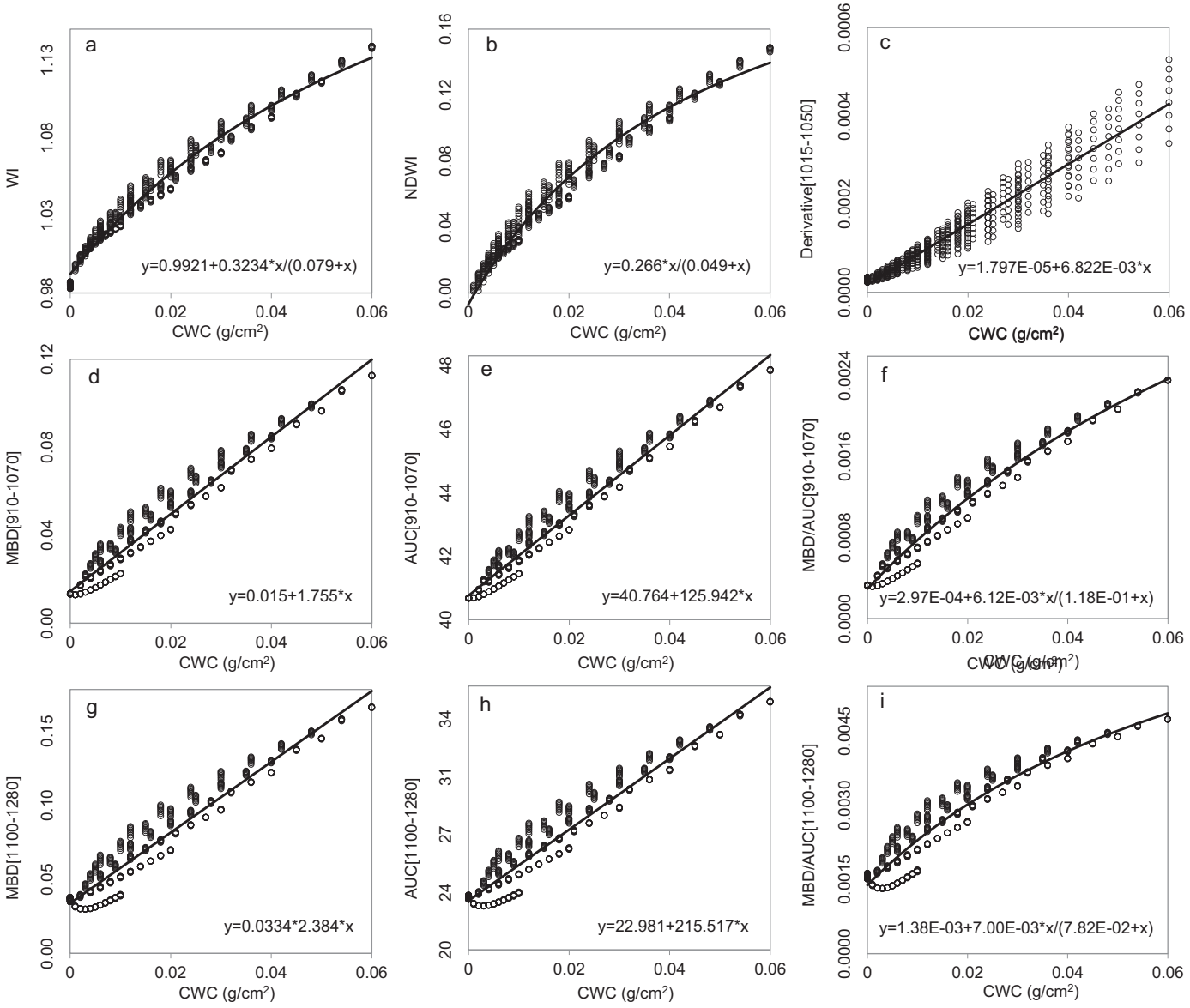

Fig. 8. Relationship between different remote sensing features and canopy water content (CWC). Lines correspond to the best fit functions.

SLC model. Simulations using SLC showed that changes in canopy reflectance due to water stress were mostly explained by leaf area index (LAI), leaf slope (LIDF*a*) and equivalent water thickness (EWT). We conclude that suitable target variables for remote sensing based assessment of water stress are LAI and canopy water content (CWC), which is defined as EWT × LAI.

Once calibrated, we used the SLC model to analyse the sensitivity of different indices and spectral absorption features to detect water stress in Tamarugo, six for detecting changes in LAI (ΔLAI) and nine for detecting changes in canopy water content (ΔCWC). The sensitivity analysis showed that the Water Index was the most sensitive RS feature to ΔCWC for low values of CWC (<0.036 g/cm^2), but its sensitivity decreased towards higher CWC values. From 0.036 g/cm^2 onwards AUC [910–1070] was the most sensitive. Derivative [1015, 1050] was the most influenced RS feature by changes in LIDF*a*, presenting an increasing scatter around the fitted curve for high values of CWC. RS features for detecting changes in LAI were generally asymptotic, showing a decreasing sensitivity to ΔLAI for LAI values higher than 1. The RVI showed a linear relationship with LAI, but also the highest sensitivity to changes in leaf slope. Considering the whole range of LAI, the $CI_{red\text{-}edge}$ performed the best, which is in agreement with results obtained by Herrmann et al. (2011) in wheat and Viña et al. (2011) in maize and soybean.

This study proved that the adaptation of Tamarugo to adjust the incidence angle for light by leaf movement can influence the results of RS based assessments. The diurnal patterns of leaf movement must be taken into consideration when using remote sensing tools for water stress assessments of this species.

Remote sensing approaches for detecting CWC changes in Tamarugo trees are limited to the hyperspectral domain, since narrow bands are needed to calculate most of the spectral features and indices proposed in literature and tested in this study. Such data can be obtained from satellite sensors like Hyperion, and airborne sensors like AVIRIS and HyMap, which are hardly ever available for this geographic area. The exception is the NDWI which can be calculated using the broad bands of the MODIS sensor at 860 and 1240 nm. However, the spatial resolution of these bands is very low (500 m), making an assessments at tree level impossible.

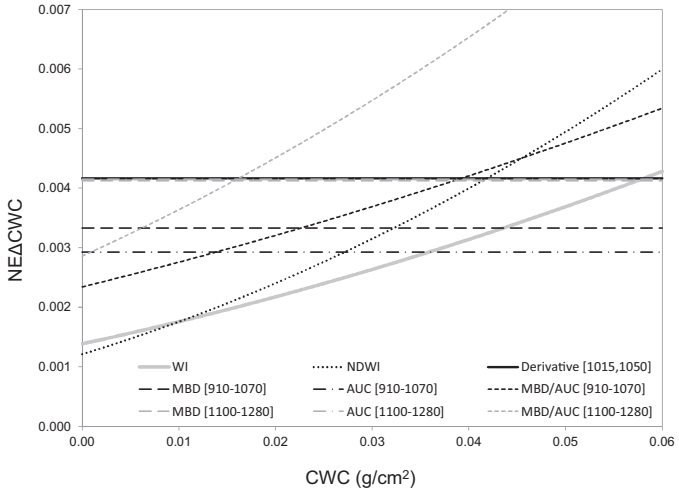

Fig. 9. Sensitivity analysis of different remote sensing features for detecting water stress in terms of changes in canopy water content (ΔCWC). The sensitivity analysis was performed using the NEΔCWC (Eq. (3)). Low values indicate high sensitivity to changes in CWC.

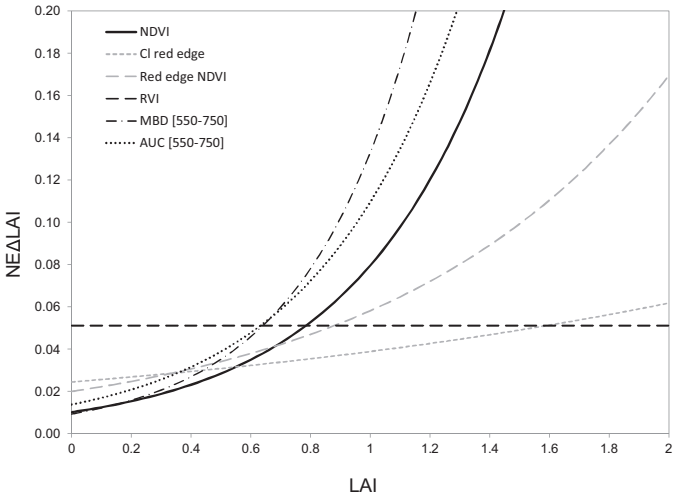

Fig. 11. Sensitivity analysis of different remote sensing features for detecting water stress in terms of changes in LAI. The sensitivity analysis was performed using the NEΔLAI (Eq. (4)). Low values indicate high sensitivity to changes in LAI.

The new generation of very high spatial resolution (VHSR) satellites seems to be very promising for detecting LAI changes in single Tamarugo trees, since they include a red-edge band at 2 m pixel resolution (WorldView2) or less (1.2 m pixel resolution for the WorldView3 satellite, expected to be launched in 2014), allowing the calculation of red-edge based vegetation indices. The WorldView3 sensor is expected to deliver also 8 bands in the SWIR region at 3.7 m pixel resolution (1195–2365 nm), opening new perspectives for canopy water estimations.

Nevertheless, due to the high cost of VHSR imagery, sensors with moderate spatial resolution like Landsat (30 m) and low spatial resolution like MODIS (250/500 m) are also a good alternative and indices like NDVI and RVI can be used considering the above mentioned limitations and scale constraints. These sensors are also interesting since they provide a long and consistent time series of images to study temporal dynamics and trends of vegetation. A key issue for assessing arid vegetation using moderate to low spatial resolution imagery is to estimate the spectral contribution of non-photosynthetic material and bare soil to the mixed pixel, since foliar spectral properties of desert plants seem to be very stable along environmental gradients (Asner et al., 2000). Therefore, species like Tamarugo would resolve water scarcity via controlling

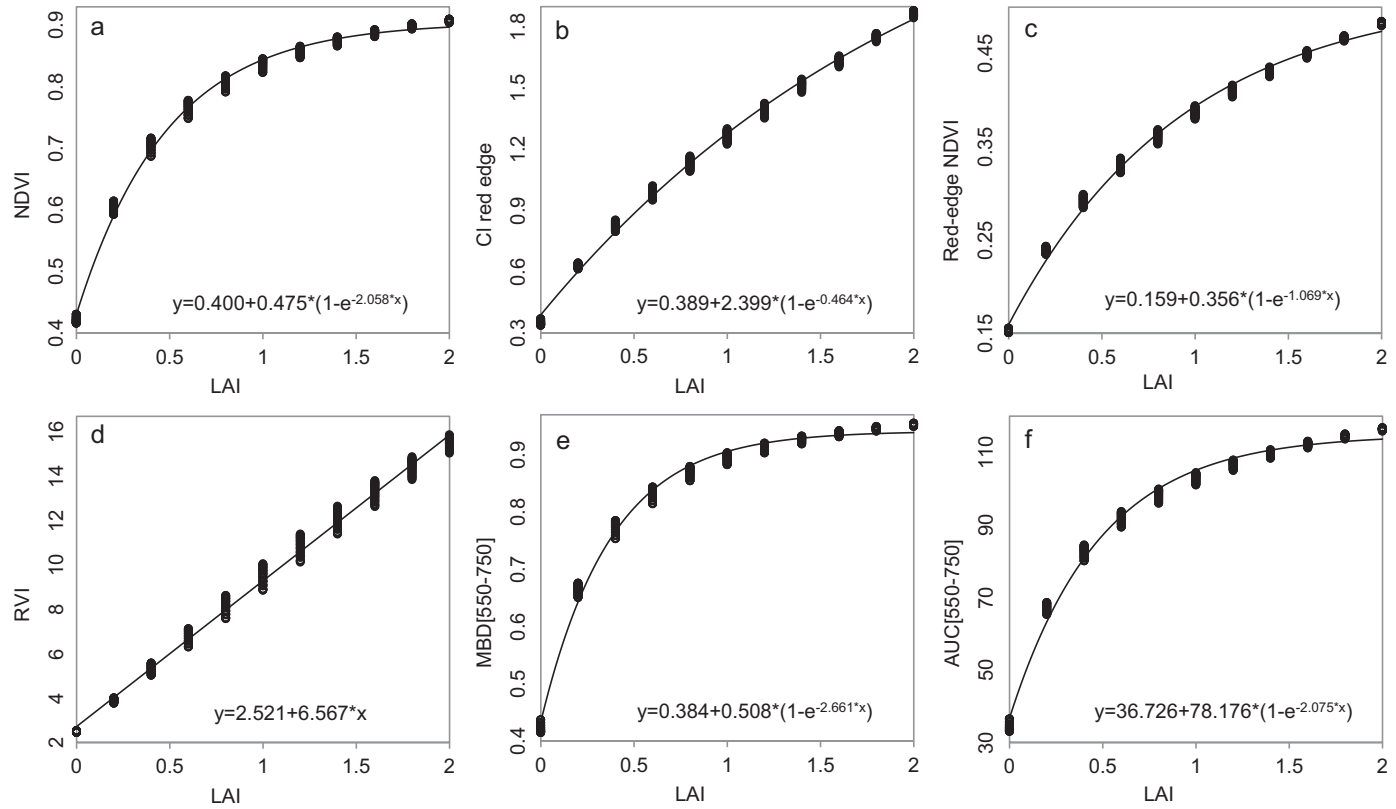

Fig. 10. Relationship between different remote sensing features and LAI. Lines correspond to the best fit functions.

biomass production rather than adjusting foliar properties, thus the green canopy fraction would be a good water stress indicator at the stand level. This would be matter for further research.

Acknowledgements

This work has been supported by CONICYT-Chile and Wageningen University. The authors would like to thank CONAF-Chile for the donation of plants for the experiment; to P. Silva, C. Pastenes and U. Arriagada (Universidad de Chile); S. Estay and E. Gayó (PUC); N. Gutiérrez (CONAF); C. Chávez and C. Baeza for providing logistical support and equipment; and to V. Laurent (WUR) for advising on the SLC simulations.

References

Acevedo, E., Ortiz, M., Franck, N., Sanguineti, P., 2007. Relaciones hídricas de Prosopis tamarugo Phil. Uso de isótopos estables. Universidad de Chile, Santiago, Chile.

Aguirre, J.J., Wrann, J., 1985. The genus prosopis and its management at the Tamarugal Pampa. In: Habit, M. (Ed.), The Current State of Knowledge on *Prosopis tamarugo*. F.A.O., Rome, pp. 3–32.

Alpert, P., Oliver, M.J., 2002. Drying without dying. In: Black, M., Pritchard, H.W. (Eds.), Desiccation and Survival in Plants: Drying Without Dying. CABI, Wallingford, UK, pp. 4–31.

Altamirano, H., 2006. *Prosopis tamarugo* Phil. Tamarugo. In: Donoso, C. (Ed.), Las especies arbóreas de los bosques templados de Chile y Argentina. Autoecología. Marisa Cuneo Ediciones, Valdivia, Chile, pp. 534–540.

Asner, G.P., 1998. Biophysical and biochemical sources of variability in canopy reflectance. Remote Sensing of Environment 64, 234–253.

Asner, G.P., Heidebrecht, K.B., 2002. Spectral unmixing of vegetation, soil and dry carbon cover in arid regions: comparing multispectral and hyperspectral observations. International Journal of Remote Sensing 23, 3939–3958.

Asner, G.P., Wessman, C.A., Bateson, C.A., Privette, J.L., 2000. Impact of tissue canopy, and landscape factors on the hyperspectral reflectance variability of arid ecosystems. Remote Sensing of Environment 74, 69–84.

Barchuk, A.H., Valiente-Banuet, A., 2006. Comparative analysis of leaf angle and sclerophylly of *Aspidosperma quebracho-blanco* on a water deficit gradient. Austral Ecology 31, 882–891.

Baret, F., Houlès, V., Guérif, M., 2007. Quantification of plant stress using remote sensing observations and crop models: the case of nitrogen management. Journal of Experimental Botany 58, 869–880.

Boochs, F., Kupfer, G., Dockter, K., Kuhbauch, W., 1990. Shape of the red edge as vitality indicator for plants. International Journal of Remote Sensing 11, 1741–1753.

Carter, G., 1993. Responses of leaf spectral reflectance to plant stress. American Journal of Botany 80, 239–243.

Carter, G., 1991. Primary and secondary effects of water content on the spectral reflectance of leaves. American Journal of Botany 78, 916–924.

Carter, G.A., Knapp, A.K., 2001. Leaf optical properties in higher plants: linking spectral characteristics to stress and chlorophyll concentration. American Journal of Botany 88, 677–684.

Clark, R.N., Roush, T.L., 1984. Reflectance spectroscopy: quantitative analysis techniques for remote sensing applications. Journal of Geophysical Research 89, 6329–6340.

Clevers, J.G.P.W., Kooistra, L., Schaepman, M.E., 2010. Estimating canopy water content using hyperspectral remote sensing data. International Journal of Applied Earth Observation and Geoinformation 12, 119–125.

Clevers, J.G.P.W., Kooistra, L., Schaepman, M.E., 2008. Using spectral information from the NIR water absorption features for the retrieval of canopy water content. International Journal of Applied Earth Observation and Geoinformation 10, 388–397.

Colombo, R., Meroni, M., Marchesi, A., Busetto, L., Rossini, M., Giardino, C., Panigada, C., 2008. Estimation of leaf and canopy water content in poplar plantations by means of hyperspectral indices and inverse modeling. Remote Sensing of Environment 112, 1820–1834.

Combal, B., Baret, F., Weiss, M., Trubuil, A., Macé, D., Pragnère, A., Myneni, R., Knyazikhin, Y., Wang, L., 2003. Retrieval of canopy biophysical variables from bidirectional reflectance using prior information to solve the ill-posed inverse problem. Remote Sensing of Environment 84, 1–15.

CONAF, 1997. In: Gobierno de Chile (Ed.), Plan de Manejo Reserva Nacional Pampa del Tamarugal. Ministerio de Agricultura, Chile, Res. 425.

Curran, P.J., 1989. Remote sensing of foliar chemistry. Remote Sensing of Environment 30, 271–278.

Curran, P.J., Dungan, J.L., Peterson, D.L., 2001. Estimating the foliar biochemical concentration of leaves with reflectance spectrometry: testing the Kokaly and Clark methodologies. Remote Sensing of Environment 76, 349–359.

Danson, F.M., Plummer, S.E., 1995. Red-edge response to forest leaf area index. International Journal of Remote Sensing 16, 183–188.

Darvishzadeh, R., Atzberger, C., Skidmore, A., Schlerf, M., 2011. Mapping grassland leaf area index with airborne hyperspectral imagery: a comparison study of statistical approaches and inversion of radiative transfer models. ISPRS Journal of Photogrammetry and Remote Sensing 66, 894–906.

Ezcurra, E., Arizaga, S., Valverde, P.L., Mourelle, C., Flores-Martínez, A., 1992. Foliole movement and canopy architecture of *Larrea tridentata* (DC.) Cov. in Mexican deserts. Oecologia 92, 83–89.

Filella, I., Penuelas, J., 1994. The red edge position and shape as indicators of plant chlorophyll content, biomass and hydric status. International Journal of Remote Sensing 15, 1459–1470.

Flexas, J., Briantais, J.M., Cerovic, Z., Medrano, H., Moya, I., 2000. Steady-state and maximum chlorophyll fluorescence responses to water stress in grapevine leaves: a new remote sensing system. Remote Sensing of Environment 73, 283–297.

Flexas, J., Escalona, J.M., Evain, S., Gulías, J., Moya, I., Osmond, C.B., Medrano, H., 2002. Steady-state chlorophyll fluorescence (Fs) measurements as a tool to follow variations of net CO2 assimilation and stomatal conductance during water-stress in C3 plants. Physiologia Plantarum 114, 231–240.

Gao, B.C., 1996. NDWI – a normalized difference water index for remote sensing of vegetation liquid water from space. Remote Sensing of Environment 58, 257–266.

Gitelson, A., Merzlyak, M.N., 1994. Spectral relfectance changes associated with autumn senescence of *Aesculus hippocastanum* L. and *Acer platanoides* L. leaves. Spectral features and relation to chlorophyll estimation. Journal of Plant Physiology 143, 286–292.

Gitelson, A.A., 2004. Wide dynamic range vegetation index for remote quantification of biophysical characteristics of vegetation. Journal of Plant Physiology 161, 165–173.

Gitelson, A.A., Keydan, G.P., Merzlyak, M.N., 2006. Three-band model for noninvasive estimation of chlorophyll, carotenoids, and anthocyanin contents in higher plant leaves. Geophysical Research Letters 33, L11402.

Govender, M., Dye, P.J., Weiersbye, I.M., Witkowski, E.T.F., Ahmed, F., 2009. Review of commonly used remote sensing and ground-based technologies to measure plant water stress. Water SA 35, 741–752.

Hapke, B., 1981. Bidirectional reflectance spectroscopy 1. Theory. Journal of Geophysical Research 86, 3039–3054.

Herrmann, I., Pimstein, A., Karnieli, A., Cohen, Y., Alchanatis, V., Bonfil, D.J., 2011. LAI assessment of wheat and potato crops by VENμS and sentinel-2 bands. Remote Sensing of Environment 115, 2141–2151.

Horler, D.N.H., Dockray, M., Barber, J., 1983. The red edge of plant leaf reflectance. International Journal of Remote Sensing 4, 273–288.

Houston, J., 2006. Evaporation in the Atacama Desert: an empirical study of spatio-temporal variations and their causes. Journal of Hydrology 3, 402–412.

Houston, J., Hartley, A.J., 2003. The central andean west-slope rainshadow and its potential contribution to the origin of hyper-aridity in the Atacama desert. International Journal of Climatology 23, 1453–1464.

Huang, Z., Turner, B.J., Dury, S.J., Wallis, I.R., Foley, W.J., 2004. Estimating foliage nitrogen concentration from HYMAP data using continuum removal analysis. Remote Sensing of Environment 93, 18–29.

Huber, S., Kneubühler, M., Psomas, A., Itten, K., Zimmermann, N.E., 2008. Estimating foliar biochemistry from hyperspectral data in mixed forest canopy. Forest Ecology and Management 256, 491–501.

Hunt Jr., E.R., Rock, B.N., 1989. Detection of changes in leaf water content using near- and middle-infrared reflectances. Remote Sensing of Environment 30, 43–54.

Jacquemoud, S., Baret, F., 1990. PROSPECT: a model of leaf optical properties spectra. Remote Sensing of Environment 34, 75–91.

Jacquemoud, S., Verhoef, W., Baret, F., Bacour, C., Zarco-Tejada, P.J., Asner, G.P., François, C., Ustin, S.L., 2009. PROSPECT + SAIL models: a review of use for vegetation characterization. Remote Sensing of Environment 113, S56–S66.

Jordan, C.F., 1969. Derivation of leaf-area index from quality of light on the forest floor. Ecology 50, 663–666.

Karnieli, A., Dall'Olmo, G., 2003. Remote-sensing monitoring of desertification, phenology, and droughts. Management of Environmental Quality 14, 22–38.

Knipling, E.B., 1970. Physical and physiological basis for the reflectance of visible and near-infrared radiation from vegetation. Remote Sensing of Environment 1, 155–159.

Kokaly, R.F., Clark, R.N., 1999. Spectroscopic determination of leaf biochemistry using band-depth analysis of absorption features and stepwise multiple linear regression. Remote Sensing of Environment 67, 267–287.

Kokaly, R.F., Despain, D.G., Clark, R.N., Livo, K.E., 2003. Mapping vegetation in Yellowstone National Park using spectral feature analysis of AVIRIS data. Remote Sensing of Environment 84, 437–456.

Laurent, V.C.E., Verhoef, W., Clevers, J.G.P.W., Schaepman, M.E., 2011a. Estimating forest variables from top-of-atmosphere radiance satellite measurements using coupled radiative transfer models. Remote Sensing of Environment 115, 1043–1052.

Laurent, V.C.E., Verhoef, W., Clevers, J.G.P.W., Schaepman, M.E., 2011b. Inversion of a coupled canopy–atmosphere model using multi-angular top-of-atmosphere radiance data: a forest case study. Remote Sensing of Environment 115, 2603–2612.

Liu, C.C., Welham, C.V.J., Zhang, X.Q., Wang, R.Q., 2007. Leaflet movement of robinia pseudoacacia in response to a changing light environment. Journal of Integrative Plant Biology 49, 419–424.

McKay, C.P., Friedmann, E.I., Gómez-Silva, B., Cáceres-Villanueva, L., Andersen, D.T., Landheim, R., 2003. Temperature and moisture conditions for life in the extreme arid region of the Atacama desert: four years of observations including the El Niño of 1997–1998. Astrobiology 3, 393–406.

Mooney, H.A., Gulmon, S.L., Rundel, P.W., Ehleringer, J., 1980. Further observations on the water relations of *Prosopis tamarugo* of the northern Atacama desert. Oecologia 44, 177–180.

Navarro-González, R., Rainey, F.A., Molina, P., Bagaley, D.R., Hollen, B.J., De La Rosa, J., Small, A.M., Quinn, R.C., Grunthaner, F.J., Cáceres, L., Gomez-Silva, B., McKay, C.P., 2003. Mars-like soils in the Atacama Desert Chile, and the dry limit of microbial life. Science 302, 1018–1021.

Pastenes, C., Pimentel, P., Lillo, J., 2005. Leaf movements and photoinhibition in relation to water stress in field-grown beans. Journal of Experimental Botany 56, 425–433.

Pastenes, C., Porter, V., Baginsky, C., Norton, P., González, J., 2004. Paraheliotropism can protect water-stressed bean (*Phaseolus vulgaris* L.) plants against photoinhibition. Journal of Plant Physiology 161, 1315–1323.

Peñuelas, J., Pinol, J., Ogaya, R., Filella, I., 1997. Estimation of plant water concentration by the reflectance Water Index WI (R900/R970). International Journal of Remote Sensing 18, 2869–2875.

Pérez-Priego, O., Zarco-Tejada, P.J., Miller, J.R., Sepulcre-Cantó, G., Fereres, E., 2005. Detection of water stress in orchard trees with a high-resolution spectrometer through chlorophyll fluorescence in-filling of the O 2-A band. IEEE Transactions on Geoscience and Remote Sensing 43, 2860–2868.

Raven, P.H., Evert, R.F., Eichhorn, S.E., 2005. Biology of Plants. Freeman, New York, NY.

Riedemann, P., Aldunate, G., Teillier, S., 2006. Flora Nativa de valor ornamental. Chile Zona Norte. Identificación y propagación Productora Gráfica Andros Ltda, Chile.

Rojas, R., Dassargues, A., 2007. Groundwater flow modelling of the regional aquifer of the Pampa del Tamarugal, northern Chile. Hydrogeology Journal 15, 537–551.

Schaepman-Strub, G., Schaepman, M.E., Painter, T.H., Dangel, S., Martonchik, J.V., 2006. Reflectance quantities in optical remote sensing-definitions and case studies. Remote Sensing of Environment 103, 27–42.

Sudzuki, F., 1985. Evironmental influence on foliar anatomy of *Prosopis tamarugo* Phil. In: Habit, M.A. (Ed.), The current state of knowledge on *Prosopis tamarugo*: papers presented at the international round table on *Prosopis tamarugo* Phil. Arica, Chile, June 11–15, 1984. FAO, Rome.

Taiz, L., Zeiger, E., 2010. Plant Physiology. Sinauer Associates, Sunderland, MA.

Trobok, S., 1985. Fruit and seed morphology of Chilean Prosopis (Fabaceae–Mimosoidae). In: Habit, M.A. (Ed.), The Current State of Knowledge on *Prosopis tamarugo*: Papers Presented at the International Round Table on *Prosopis tamarugo* Phil. Arica, Chile, June 11–15, 1984. FAO, Rome.

Tucker, C.J., 1979. Red and photographic infrared linear combinations for monitoring vegetation. Remote Sensing of Environment 8, 127–150.

Verhoef, W., 1984. Light scattering by leaf layers with application to canopy reflectance modeling: the SAIL model. Remote Sensing of Environment 16, 125–141.

Verhoef, W., Bach, H., 2007. Coupled soil-leaf-canopy and atmosphere radiative transfer modeling to simulate hyperspectral multi-angular surface reflectance and TOA radiance data. Remote Sensing of Environment 109, 166–182.

Verhoef, W., Bach, H., 2003. Simulation of hyperspectral and directional radiance images using coupled biophysical and atmospheric radiative transfer models. Remote Sensing of Environment 87, 23–41.

Viña, A., Gitelson, A.A., 2005. New developments in the remote estimation of the fraction of absorbed photosynthetically active radiation in crops. Geophysical Research Letters 32, 1–4.

Viña, A., Gitelson, A.A., Nguy-Robertson, A.L., Peng, Y., 2011. Comparison of different vegetation indices for the remote assessment of green leaf area index of crops. Remote Sensing of Environment 115, 3468–3478.

Vohland, M., Mader, S., Dorigo, W., 2010. Applying different inversion techniques to retrieve stand variables of summer barley with PROSPECT + SAIL. International Journal of Applied Earth Observation and Geoinformation 12, 71–80.

Zarco-Tejada, P.J., Rueda, C.A., Ustin, S.L., 2003. Water content estimation in vegetation with MODIS reflectance data and model inversion methods. Remote Sensing of Environment 85, 109–124.